




Ion-Implanted Epitaxially Grown Gd_2O_3 on Silicon with Improved Electrical Properties

A. JOSEPH ^{1,2,4} G. LILIENKAMP,³ T.F. WIETLER,¹ and H.J. OSTEN¹

1.—Institute of Electronic Materials and Devices, Leibniz Universität Hannover, Schneiderberg 32, 30167 Hannover, Germany. 2.—Hannover School for Nanotechnology, Leibniz Universität Hannover, Schneiderberg 39, 30167 Hannover, Germany. 3.—Clausthal University of Technology (TU Clausthal), Adolph-Roemer-Straße 2A, 38678 Clausthal-Zellerfeld, Germany. 4.—e-mail: anitjoseph3@gmail.com

The effects of nitrogen incorporation by high-dose ion implantation in epitaxial gadolinium oxide (Gd_2O_3) films on Si (111) followed by annealing have been investigated. The nitrogen content in the oxide layer was changed by altering the implantation dose. The presence of nitrogen incorporation on the Gd_2O_3 layer was studied using Auger electron spectroscopy. Nitrogen incorporation is believed to occur by filling the oxygen vacancies or by removing hydroxyl group ions in Gd_2O_3 . A maximum concentration of 11% was obtained for nitrogen in the interface between the silicon dioxide and Gd_2O_3 layer and the implanted areas of the Gd_2O_3 oxide layer after sputter depth profiling. The nitrogen distribution in the layer was found to be non-uniform. Nitrogen incorporation sharply reduced the leakage current and effectively suppressed the hysteresis. Leakage current was two orders lower compared with the pure Gd_2O_3 .

Key words: Ion implantation, nitrogen concentration, epitaxial growth, oxynitrides, leakage current

INTRODUCTION

Due to high direct tunnelling current,¹ silicon dioxide thinner than 1.5 nm cannot be used for the gate dielectric of complementary metal oxide semiconductor (CMOS) devices.² High-dielectric-constant (high- k) oxides offer an alternative to silicon dioxide (SiO_2) in very-large-scale integrated (VLSI) devices. The basic concept of using high-dielectric-constant materials is increasing the film thickness to reduce the tunnelling leakage current and improve reliability, while scaling the capacitance equivalent oxide thickness (CET) below the direct tunnelling limit of SiO_2 .³ Rare earth oxides (REOs) have received much attention due to their many advantages, including high dielectric constant,^{4–6} sufficiently high breakdown strength, extremely low leakage current, and well-behaved interface

properties. REOs^{7,8} such as La_2O_3 ,⁹ and Gd_2O_3 ,¹⁰ have been studied in detail. Also, the epitaxial growth of crystalline Gd_2O_3 on silicon in the cubic *bixbyite* structure has been widely investigated.¹¹ This material has a large band gap of about 6 eV and nearly symmetrical band offsets, as well as a low lattice mismatch of about -0.4% to Si.¹² Layers grown by an optimized process can display a sufficiently high- k value to achieve equivalent oxide thickness (EOT) values below 1 nm, combined with ultra-low leakage current densities, excellent reliability, and high electrical breakdown voltages. A variety of metal oxide semiconductor (MOS) devices have been fabricated based on these layers.¹³

The current field of research into rare earth nitrides (RENs) is rapidly expanding, driven by the material needs of proposed electronic and spintronic devices. The importance of RENs has been established due to their semiconducting and ferromagnetic properties. The present enthusiasm for the capability of spintronic devices has increased the

(Received March 22, 2020; accepted August 1, 2020;
published online August 14, 2020)

urgency of investigating intrinsic ferromagnetic semiconductors, of which the RENs offer a rich arrangement of illustrations.¹⁴ It is exciting to explore more about the transition between these two materials (i.e. REOs and RENs), which form rare earth oxynitrides. Only a few research publications about gadolinium oxynitrides are available, and the concentration of nitrogen has not been studied in detail.¹⁵

In addition, ionic oxides generally have abundant oxygen vacancies (V_{OS}). Considering different high- k oxides (e.g., HfO_2 , ZrO_2), ab initio calculations suggest that the presence of V_{OS} is associated with the degradation of electrical properties.^{16,17} Different methods have been suggested to enhance the electrical properties of high- k oxide thin films, among which dopant incorporation has been found effective. It is reported that the inclusion of nitrogen significantly improves the electrical properties in various oxides.^{18–20} Ayan et al.²¹ reported that incorporating a small amount of nitrogen during the growth of epitaxial Gd_2O_3 thin films improved the electrical properties.

In this work, we fabricated gadolinium oxynitride layers using high-dose nitrogen implantation into Gd_2O_3 layers grown by molecular beam epitaxy (MBE). The obtained layers were characterized structurally using x-ray diffraction (XRD), transmission electron microscopy (TEM), and Raman spectroscopy. The nitrogen incorporation and the impact on band structure were evaluated using x-ray photoelectron spectroscopy (XPS) and have been reported.²²

We aimed to determine the nitrogen concentration in the layer using sputter depth profiling in an Auger electron spectroscopy (AES) system and investigated the changes in the electrical properties of the layer due to nitrogen incorporation.

EXPERIMENT

The samples were prepared using the MBE technique.²³ The process flow of sample preparation, nitrogen ion implantation, and the conditions were elaborated in a previous publication.²² To perform electrical characterization, platinum (Pt) metal contacts were deposited on the implanted layers. The samples were characterized electrically by measuring their room temperature leakage current versus voltage (I - V) characteristics using a semiconductor parameter analyzer (Agilent 4156C). The hysteresis of the samples was studied by capacitance-voltage (C - V) measurements using an impedance analyzer (Agilent 4294A).

An AES technique, in conjunction with ion sputtering, was used to obtain elemental concentrations in high-dose nitrogen-implanted samples. For the depth profiling process, we used a high-dose (2×10^{17} atom/ cm^2) nitrogen-implanted sample with 20 nm SiO_2 and 120 nm Gd_2O_3 , which was annealed at 800°C in N_2 ambient for 1 min.

Sputtering details: Ion: Ar+, Energy: 4 keV, Angle: 38.8° angle of incidence to the surface normal, Beam current: $\sim 1 \mu\text{A}$.

RESULTS AND DISCUSSION

In this section, we summarize our findings for the samples obtained after different processing steps. XRD measurements were employed first. XRD data do not exhibit additional phases, but we observed a drop in the intensity and broadening of the oxide peak after implantation, which may be attributed to the reduction in the thickness of the crystalline oxide layer (Fig. 1). The strain effects in the Gd_2O_3 layer may also be a reason for peak broadening, which reduces after rapid thermal annealing (RTA).

The TEM image in Fig. 2 shows a very rough surface, and strong implantation effects are observed in the upper portion of the oxide layer, whereas the effects are comparatively weak near the substrate. These findings agree well with the stopping range of ions in matter (SRIM) implantation profile and with the structure of GdN reported by McKenzie et al.²⁴ We observed the presence of an interfacial layer of thickness ~ 7 nm which formed due to annealing after implantation.²⁵

The concentration of nitrogen in the interface between the SiO_2 and Gd_2O_3 layer and the implanted areas of the Gd_2O_3 oxide layer after sputter depth profiling is summarized in Table I. The atomic percentages of all elements were obtained from the Auger spectra, depicted in Fig. 3. Because the sputtering rate for Gd_2O_3 is not known, we plotted the depth distribution as a function of sputtering time, illustrated in Fig. 4.

The quantitative Auger method calculations are on the assumption that:

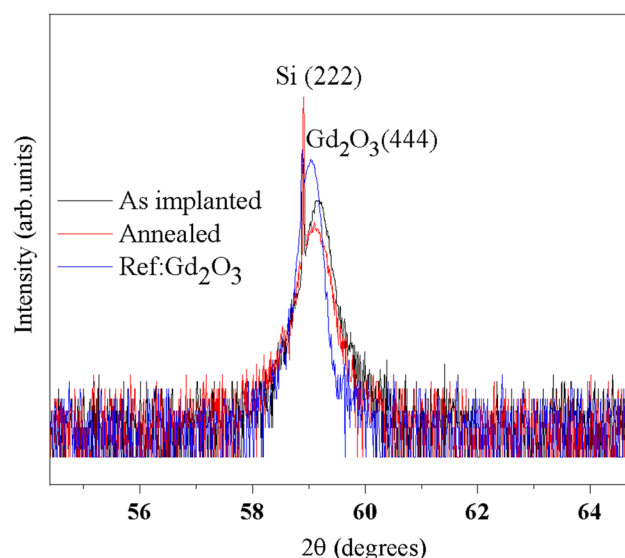


Fig. 1. X-ray diffraction pattern of ref. Gd_2O_3 sample, as-implanted and after annealing steps (all patterns were normalized to the Si (222) peak).

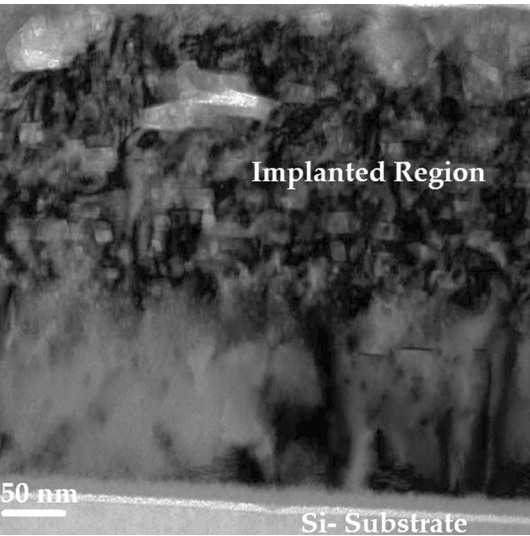


Fig. 2. TEM bright-field image analysis of the sample with the highest implantation dose.

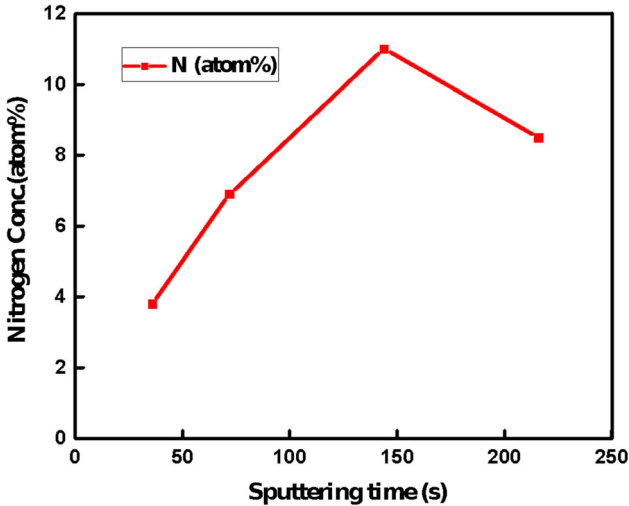


Fig. 4. Graph-sputtering time versus nitrogen concentration.

Table I. Concentration of Gd, O and N at different sputtering time

Sputtered region	Sputtering time (s)	Gd (at.%)	O (at.%)	N (at.%)	Ar (at.%)
SiO ₂	360	54.7	39.9	5.2	—
Gd ₂ O ₃	36	54.1	39.8	3.8	2.3
	72	50.7	40.2	6.9	2.2
	144	49.5	37.2	11.0	2.2
	216	48.9	39.9	8.5	2.7

Numbers in bold indicate maximum nitrogen concentration obtained

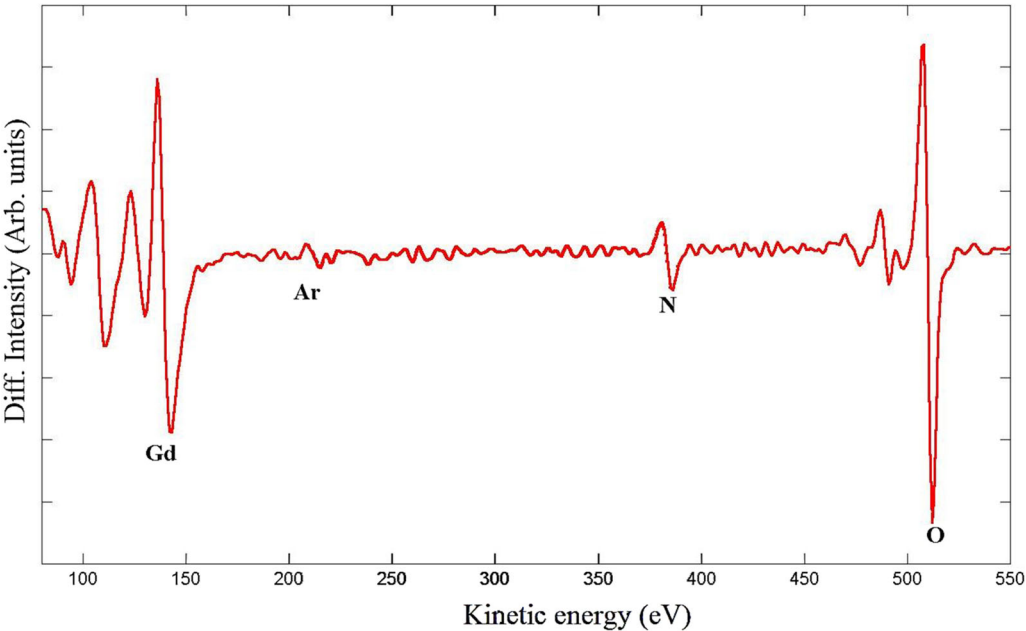


Fig. 3. Auger spectra after 72 s sputtering of the Gd₂O₃ layer. Elements present in the layer are marked in bold letters.

$$I_{A.} = S_{A.}N_{A.}, \quad (1)$$

where $I_{A.}$ is the measured Auger current from element A, $S_{A.}$ is the Auger sensitivity factor of element A, and $N_{A.}$ is the number density of atoms of type A.

If the sample contains two elements A and B, the expression gives the number density $N_{A.}$ of A²⁶:

$$N_A = \frac{\frac{I_A}{S_A}}{\frac{I_A}{S_A} + \frac{I_B}{S_B}}. \quad (2)$$

We calculated the elemental concentration using Eq. 2.

To find out nitrogen concentration N_{nitro}

$$= \frac{\frac{I_{\text{nitro}}}{S_{\text{nitro}}}}{\frac{I_{\text{nitro}}}{S_{\text{nitro}}} + \frac{I_{\text{Gd}}}{S_{\text{Gd}}} + \frac{I_{\text{Oxy}}}{S_{\text{Oxy}}} + \frac{I_{\text{Ar}}}{S_{\text{Ar}}}} \quad (3)$$

The main observation during sputter depth profiling is that the nitrogen distribution in the oxide layer is non-uniform. It takes 360 s to remove 20 nm SiO₂. The sputtering rate of SiO₂ is 3.33 nm/min. The concentration of nitrogen on the surface of the Gd₂O₃ layer seems to be around 5 at.%. Going deeper into the Gd₂O₃ layer, we obtain a maximum nitrogen concentration of 11 at.%. According to the SRIM ion distribution profile, the ion range is at 46.7 nm.²² The concentration of oxygen decreases with increasing nitrogen content, which can be explained as a result of preferential oxygen sputtering.²⁷

Electrical Characterization

The effect of nitrogen ion implantation on the dc leakage conduction of the epitaxially grown Gd₂O₃ thin films was investigated by standard I - V measurements shown in Fig. 5. At applied electric fields below 1 MV/cm, the leakage current density of the high-dose nitrogen-implanted epitaxially grown Gd₂O₃ samples were found to be about two orders of magnitude lower than the Gd₂O₃ samples grown

under similar oxygen partial pressure (PO₂). A previous publication from the same group reports that Gd₂O₃ layers grown at PO₂ $\sim 5 \times 10^{-6}$ mbar show leakage current of the order 10^{-2} A/cm², whereas the same partial pressure in nitrogen ambient growth (PN₂O $\sim 5 \times 10^{-6}$ mbar) gave leakage current in the range of 10^{-3} A/cm².²¹ For our high-dose nitrogen-implanted sample (Fig. 5), leakage current density reduced sharply to 1.8×10^{-4} A/cm².

To elucidate the enhanced electrical properties of nitrogen-implanted Gd₂O₃ layers, we have to take into account the effect of nitrogen in the electrically active defects present in Gd₂O₃. In complex oxides grown at a higher temperature, V_Os are the dominant electrically active defect sites.^{28,29} Reports show that the presence of V_Os that induce an electron conduction path and the migration of V_Os in the large electric field are the two main reasons for the enhanced leakage current density in complex oxides.^{17,30-35} When nitrogen is incorporated in the oxide layer, nitrogen atoms occupy the oxygen vacant sites and therefore change their energy levels and also immobilize the V_Os, which may successively reduce the leakage current due to the movement of the V_Os.³⁶

Further, we investigated the impact of nitrogen incorporation on the C-V behaviour of the nitrogen-implanted epitaxially grown Gd₂O₃ layers. Figure 6 depicts the C-V hysteresis characteristics of high-dose nitrogen-implanted Gd₂O₃. Reports show that C-V of a pure Gd₂O₃ sample grown at lower P_{O2} ($\sim 2 \times 10^{-7}$ mbar) exhibits strong hysteresis.³⁷ As shown in Fig. 6, nitrogen implantation in Gd₂O₃ already results in nearly ideal dielectric behaviour because of the possibility to reduce the effect of mobile oxide charges formed from the V_Os.

CONCLUSION

Nitrogen concentrations in high-dose-implanted samples were obtained using AES, in conjunction with ion sputtering. By conducting sputter depth

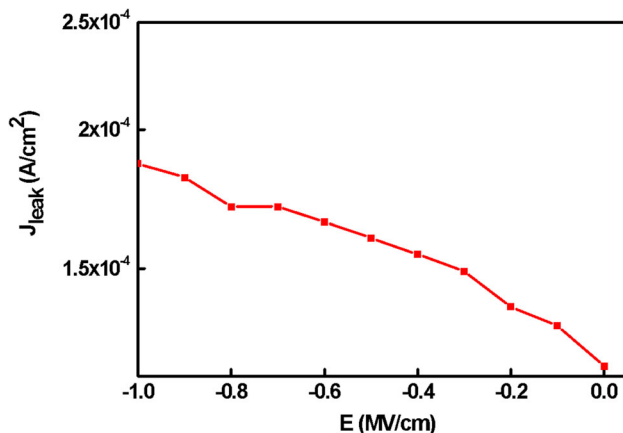


Fig. 5. Room temperature leakage current density of nitrogen-implanted Gd₂O₃.

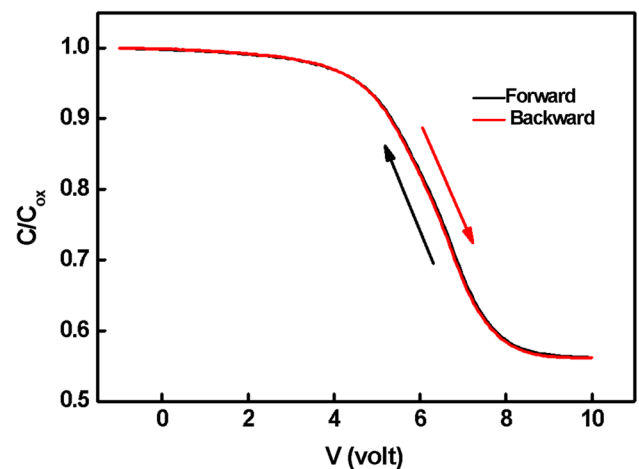


Fig. 6. C-V hysteresis of nitrogen-implanted epitaxial Gd₂O₃.

profiling, we obtained a maximum concentration of 11 at.% nitrogen in the Gd_2O_3 layer, which was not in complete agreement with the SRIM implantation profile. Ion implantation caused damage to the layer, and there were no other prominent structural changes in XRD. For uniform nitrogen distribution in the oxide layer, we need further work on implantation parameters.

Nitrogen ion implantation is an effective method for reducing leakage current and enhancing the electrical behaviour of rare earth oxides.

ACKNOWLEDGMENTS

A.J. would like to thank the Hannover School for Nanotechnology (HSN) for a fellowship. Thanks to TU Clausthal for Auger electron spectroscopy characterization and Helmholtz-Zentrum Dresden-Rossendorf e.V., a member of the Helmholtz Association for ion implantation. We also thank the Laboratory of Nano and Quantum Engineering (LNQE) of the Leibniz Universität Hannover.

FUNDING

Open Access funding provided by Projekt DEAL.

CONFLICT OF INTEREST

The authors declare that they have no conflict of interest.

OPEN ACCESS

This article is licensed under a Creative Commons Attribution 4.0 International License, which permits use, sharing, adaptation, distribution and reproduction in any medium or format, as long as you give appropriate credit to the original author(s) and the source, provide a link to the Creative Commons licence, and indicate if changes were made. The images or other third party material in this article are included in the article's Creative Commons licence, unless indicated otherwise in a credit line to the material. If material is not included in the article's Creative Commons licence and your intended use is not permitted by statutory regulation or exceeds the permitted use, you will need to obtain permission directly from the copyright holder. To view a copy of this licence, visit <http://creativecommons.org/licenses/by/4.0/>.

REFERENCES

1. H.S. Momose, S. Nakamura, T. Ohguro, T. Yoshitomi, E. Morifuji, T. Morimoto, Y. Katsumata, and H. Iwai, *IEEE Trans. Electron Devices* 45, 691 (1998).
2. J.L. Zhang, J.S. Yuan, Y. Ma, and S. Oates, *Solid State Electron.* 45, 373 (2001).
3. H.H. Ko, L.B. Chang, M.J. Jeng, P.Y. Kuei, and K.Y. Horng, *Jpn. J. Appl. Phys.* 44, 3205 (2005).
4. A.K. Jonsson, G.A. Niklasson, and M. Veszelei, *Thin Solid Films* 402, 242 (2002).
5. D.O. Lee, P. Roman, C.T. Wu, P. Mumbauer, M. Brubaker, R. Grant, and J. Ruzyllo, *Solid State Electron.* 46, 1671 (2002).
6. Y.C. Quan, J.E. Lee, H. Kang, Y. Roh, D. Jung, and C.W. Yang, *Jpn. J. Appl. Phys.* 41, 6904 (2002).
7. Y. Zhang, A. Navrotsky, H. Li, L. Li, L.L. Davis, and D.M. Strachan, *J. Non-Cryst. Solids* 296, 93 (2001).
8. L. Kang, B.H. Lee, W.J. Qi, Y. Jeon, R. Nich, S. Gopalan, K. Onishi, and J.C. Lee, *IEEE Electron. Device Lett.* 21, 181 (2000).
9. A. Chin, Y.H. Wu, S.B. Chen, C.C. Liao, and W.J. Chen, in *Symposium on VLSI Technology* (2000), p. 16.
10. J.K. Yang, M.G. Kang, and H.H. Park, *Thin Solid Films* 420–421, 571 (2002).
11. H.J. Osten, A. Laha, M. Czernohorsky, E. Bugiel, R. Dargis, and A. Fissel, *Phys. Status Solidi (a)* 205, 695 (2008).
12. M. Badylevich, S. Shamuilia, V.V. Afanas'ev, A. Stesmans, A. Laha, H.J. Osten, and A. Fissel, *Appl. Phys. Lett.* 90, 252101 (2007).
13. M.C. Lemme, H.D.B. Gottlob, T.J. Echtermeyer, M. Schmidt, H. Kurz, R. Endres, U. Schwalke, M. Czernohorsky, D. Tetzlaff, and H.J. Osten, *J. Vac. Sci. Technol.* B27, 258 (2009).
14. F. Natali, B.J. Ruck, N.O.V. Plank, H.J. Trodahl, S. Granville, C. Meyer, and W.R.L. Lambrecht, *Prog. Mater. Sci.* 58, 1316 (2013).
15. J.C. Wang, Y.R. Ye, Y.H. Wu, C.F. Ai, and W.F. Tsai, *Int. J. Nanotechnol.* 11, 135 (2014).
16. K. Xiong, J. Robertson, and S.J. Clark, *J. Appl. Phys.* 99, 044105 (2006).
17. K. Tse, D. Liu, K. Xiong, and J. Robertson, *Microelectron. Eng.* 84, 2028 (2007).
18. C.H. Choi, S.J. Rhee, T.S. Jeon, N. Lu, J.H. Sim, R. Clark, M. Niwa, and D.L. Kwong, in *Technical Digest—International Electron Devices Meeting* (2003), p. 857.
19. X.B. Lu, Z.G. Liu, Y.P. Wang, Y. Yang, X.P. Wang, H.W. Zhou, and B.Y. Nguyen, *J. Appl. Phys.* 94, 1229 (2003).
20. C.S. Kang, H.J. Cho, K. Onishi, R. Nieh, R. Choi, S. Gopalan, S. Krishnan, J.H. Han, and J.C. Lee, *Appl. Phys. Lett.* 81, 2593 (2002).
21. A.R. Chaudhuri, A. Fissel, and H.J. Osten, *J. Appl. Phys.* 113, 184108 (2013).
22. A. Joseph, D. Tetzlaff, J. Schmidt, R. Böttger, T.F. Wietler, and H.J. Osten, *J. Appl. Phys.* 120, 144103 (2016).
23. M. Czernohorsky, A. Fissel, E. Bugiel, O. Kirfel, and H.J. Osten, *Appl. Phys. Lett.* 88, 152905 (2006).
24. W.R. McKenzie, P.R. Munroe, F. Budde, B.J. Ruck, S. Granville, and H.J. Trodahl, *Curr. Appl. Phys.* 6, 407 (2006).
25. M. Czernohorsky, D. Tetzlaff, E. Bugiel, R. Dargis, H.J. Osten, H.D.B. Gottlob, M. Schmidt, M.C. Lemme, and H. Kurz, *Semicond. Sci. Technol.* 23, 035010 (2008).
26. L.C. Feldman and J.W. Mayer, *Fundamentals of Surface and Thin Film Analysis* (Upper Saddle River: Prentice Hall, 1986).
27. T. Mizutani, *Jpn. J. Appl. Phys.* 30, L628 (1991).
28. J. Robertson, K. Xiong, S.J. Clark, and S.J. Clark, *Defects in High-k Gate Dielectric Stacks NATO Science Series*, Vol. 220, ed. E. Gusev (Dordrecht: Springer, 2006), p. 175.
29. S. Guha and V. Narayanan, *Phys. Rev. Lett.* 98, 196101 (2007).
30. R.M. Fleming, D.V. Lang, C.D.W. Jones, M.L. Steigerwald, D.W. Murphy, G.B. Alers, Y.-H. Wong, R.B. van Dover, J.R. Kwo, and A.M. Sergent, *J. Appl. Phys.* 88, 850 (2000).
31. P. Broqvist and A. Pasquarello, *Appl. Phys. Lett.* 89, 262904 (2006).
32. K. Xiong and J. Robertson, *Appl. Phys. Lett.* 95, 022903 (2009).
33. D. Liu, S.J. Clark, and J. Robertson, *Appl. Phys. Lett.* 96, 032905 (2010).

- 34. R. Meyer, R. Liedtke, and R. Waser, *Appl. Phys. Lett.* 86, 112904 (2005).
- 35. J. Wang and S. Trolier-McKinstry, *Appl. Phys. Lett.* 89, 172906 (2006).
- 36. N. Umezawa, K. Shiraishi, T. Ohno, H. Watanabe, T. Chikyow, K. Torii, K. Yamabe, K. Yamada, H. Kitajima, and T. Arikado, *Appl. Phys. Lett.* 86, 143507 (2005).
- 37. A.R. Chaudhuri, A. Fissel, V.R. Archakam, and H.J. Osten, *Appl. Phys. Lett.* 102, 022904 (2013).

Publisher's Note Springer Nature remains neutral with regard to jurisdictional claims in published maps and institutional affiliations.